Available online at www.sciencedirect.com
ScienceDirect
Thin Solid Films 515 (2007) 7313 – 7317
www.elsevier.com/locate/tsf

Reduction of sidewall roughness, insertion loss and crosstalk of polymer arrayed waveguide grating using vapor-redissolution technique

Hai-Ming Zhang [a], Chun-Sheng Ma [a], Zhen-Kun Qin [a,b], Xi-Zhen Zhang [a], Dan-Zhang [a], Shi-Yong Liu [a], Da-Ming Zhang [a,c,*]

[a] State Key Laboratory on Integrated Optoelectronics, College of Electronic Science and Engineering, Jilin University, 2699 Qianjin Street, Changchun 130012, China
[b] Jilin Normal University, Siping 136000, China
[c] State Key Laboratory on Applied Optics, Changchun Institute of Optics, Fine Mechanics and Physics, Chinese Academy of Sciences, Changchun 130021, China

Received 9 March 2006; received in revised form 14 January 2007; accepted 13 February 2007
Available online 23 February 2007

Abstract

An efficient vapor-redissolution technique is used to greatly reduce sidewall scattering loss in the polymer arrayed waveguide grating (AWG) fabricated on a silicon substrate. Smoother sidewalls are achieved and verified by a scanning electron microscopy. Reduction of sidewall scattering loss is further measured for the loss measurement of both straight waveguides and AWG devices. The sidewall loss in straight polymer waveguide is decreased by 2.1 dB/cm, the insertion loss of our AWG device is reduced by about 5.5 dB for the central channel and 6.7 dB for the edge channels, and the crosstalk is reduced by 2.5 dB after the vapor-redissoluton treatment.

Keywords: Arrayed waveguide grating; Vapor-redissolution; Insertion loss; Crosstalk

1. Introduction

Wavelength-division multiplexing (WDM) technique is considered as a promising solution to meet the demand of tremendous information transmission in the current telecommunication network, because it expands the network's capacity and also offers flexibility for the construction of network architectures. AWGs are key devices in WDM systems in which they can serve as multiplexers, demultiplexers and wavelength routers [1–4]. Furthermore, AWGs can be constructed as planar lightwave circuits and can be manufactured and packaged by using standard low-cost techniques, thus enabling to cover mass market applications [5]. The loss of an AWG device comes from material absorption loss, sidewall roughness scattering, leakage loss, coupling loss, and bending loss. Previous researches show that the loss of AWG primarily results from sidewall roughness or imperfection except for material absorption loss, which scatters the guided wave into radiated modes [6]. This loss mechanism greatly affects the performance of AWG devices fabricated by silica-on-silicon, III–V semiconductors, $LiNbO_3$, silicon-on-insulator, and polymers. To solve this problem, a laser method to greatly reduce the surface roughness of a silica microdisk has been developed [7].

During the last 15 years polymer AWG devices have been proposed and demonstrated because they provide such advantages as lower cost, simpler film preparation, and easier control of the refractive index, compared with other kinds of AWG multiplexers [8,9]. Like devices made in other materials, the sidewall roughness scattering is also the main loss factor for polymer ones. A thermal-flow technique to reduce the sidewall roughness have demonstrated its effectiveness in reducing the waveguide loss has been reported [10].

In this paper, an efficient vapor-redissolution (VRD) technique for reducing the sidewall roughness and waveguide

* Corresponding author. College of Electronic Science and Engineering, State Key Laboratory on Integrated Optoelectronics, Jilin University, 2699 Qianjin Street, Changchun 130012, China. Tel.: +86 431 5168244 8213; fax: +86 431 5168270.
E-mail address: zhangdmm@263.net (D.-M. Zhang).

0040-6090/$ - see front matter © 2007 Elsevier B.V. All rights reserved.
doi:10.1016/j.tsf.2007.02.068

loss is reported. Furthermore, we provide experimental evidence to show that this simple technique can reduce the insertion loss and the crosstalk of the fabricated AWG device by 5.5–6.7 dB and 2.5 dB, respectively.

2. Experimental details

We have previously demonstrated polymer AWG devices fabricated by the method of metal mask incorporating reactive ion etching (RIE) technique [11]. This method can be applied to a wide range of polymer waveguide devices fabricated by epoxy, acrylic polymers, polyimide, polystyrene, polymethylmethacrylate, poly(vinyl ether), and so on. In this paper, we select the 2,3,4,5,6-pentafluorostyrene-co-glycidylmethacrylate (PFS-co-GMA) as the polymer material. And the molecular formula of the PFS-co-GMA is shown in Fig. 1, whose glass transition temperature is about 102–107 °C. The styrene is used to regulate the PFS-co-GMA to form the core material with higher refractive index. So the refractive index can be varied over a relatively large range, i.e. a range of 1.461–1.555. We select the refractive index difference Δ=0.5% between the core and the cladding (Fig. 2). We fabricate buried channel waveguides with the fluoropolymer material by spin-coating, photolithography, and RIE techniques. The schematic diagram of the fabrication procedures is drawn in Fig. 3, which includes (a) spin-coating the lower cladding and core layer, (b) photolithography, (c) RIE, (d) VRD, and (e) spin-coating the upper cladding. Reduplicating experiments we find that the sidewall roughness of the waveguide mainly come from four factors, which include nonhomogeneity of photolithography, roughness of mask, incomplete developing and side-etching in the RIE process. The VRD process is performed after the waveguide cores are formed by the RIE. In this process, samples are placed into the saturated solvent vapor under various temperatures for different durations. By means of the action of saturated vapor pressure, solvent molecules adsorb and get into sidewalls of waveguides and enhance their fluidity. Then, the surface tension of sidewalls smoothes their corrugation. We select the tetrahydrofuran (THF) as the solvent in the VRD process in our experiment. In order to control the VRD speed and without significantly changing the shape of the square waveguide, vapor temperatures are chosen within 50–60 °C

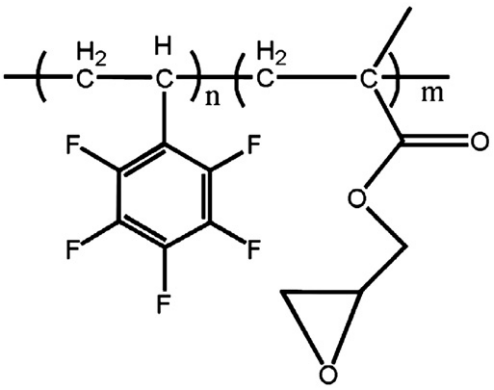

Fig. 1. Molecular formula of the PFS-co-GMA.

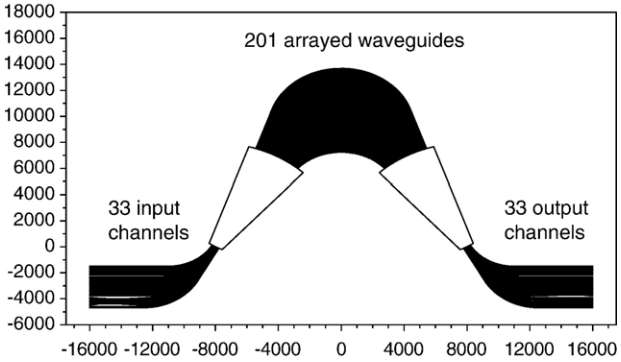

Fig. 2. Schematic layout of the designed AWG device.

(17–7 °C below its boiling point of 67 °C). For better comparison, we use a template with three identical AWG figures to fabricate three duplicated AWG samples at a time, which preserve the same sidewall roughness. These samples are then vapor-redissolved by using different vapor temperatures and times. Scanning electron microscopy (SEM) characterization shows the significantly reduced sidewall roughness after the VRD process in Fig. 4. Fig. 4a and b shows the initial AWG waveguides before vapor-redissolving, Fig. 4c and d after 45 °C vapor-redissolving for 45 min, and Fig. 4e and f after 55 °C vapor-redissolving for 35 min. Within our examined temperature range of 15–65 °C, higher temperature and longer redissolving time lead to smoother sidewalls. As shown in Fig. 4b, d and f, we can find that the VRD process also deforms waveguide shapes. The waveguide shapes are obtained after vapor-redissolving at different temperatures and times. The original shape of the waveguide before vapor-redissolving is quadrate 5×5 μm^2. The VRD of the samples rounds off the waveguide corners and increases its base width. This deformation changes slightly the effective refractive index of the guide core, which determines the AWG's wavelengths, free spectra range (FSR), and bandwidth [12]. However, we can see from these SEM photographs that the slight deformation is not

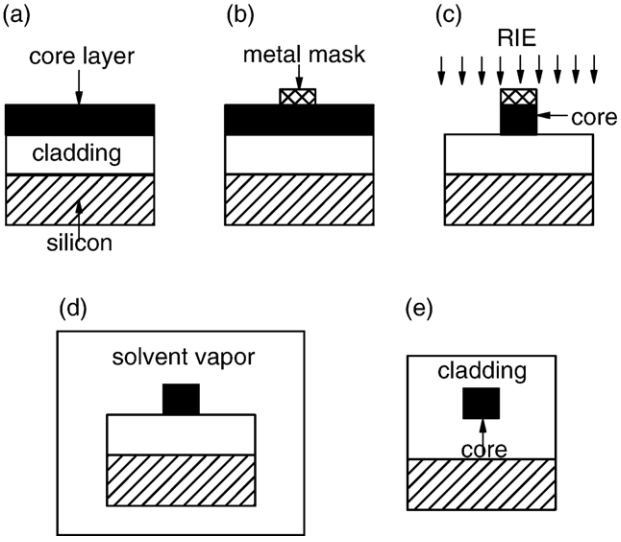

Fig. 3. Schematic diagram of the fabrication procedures.

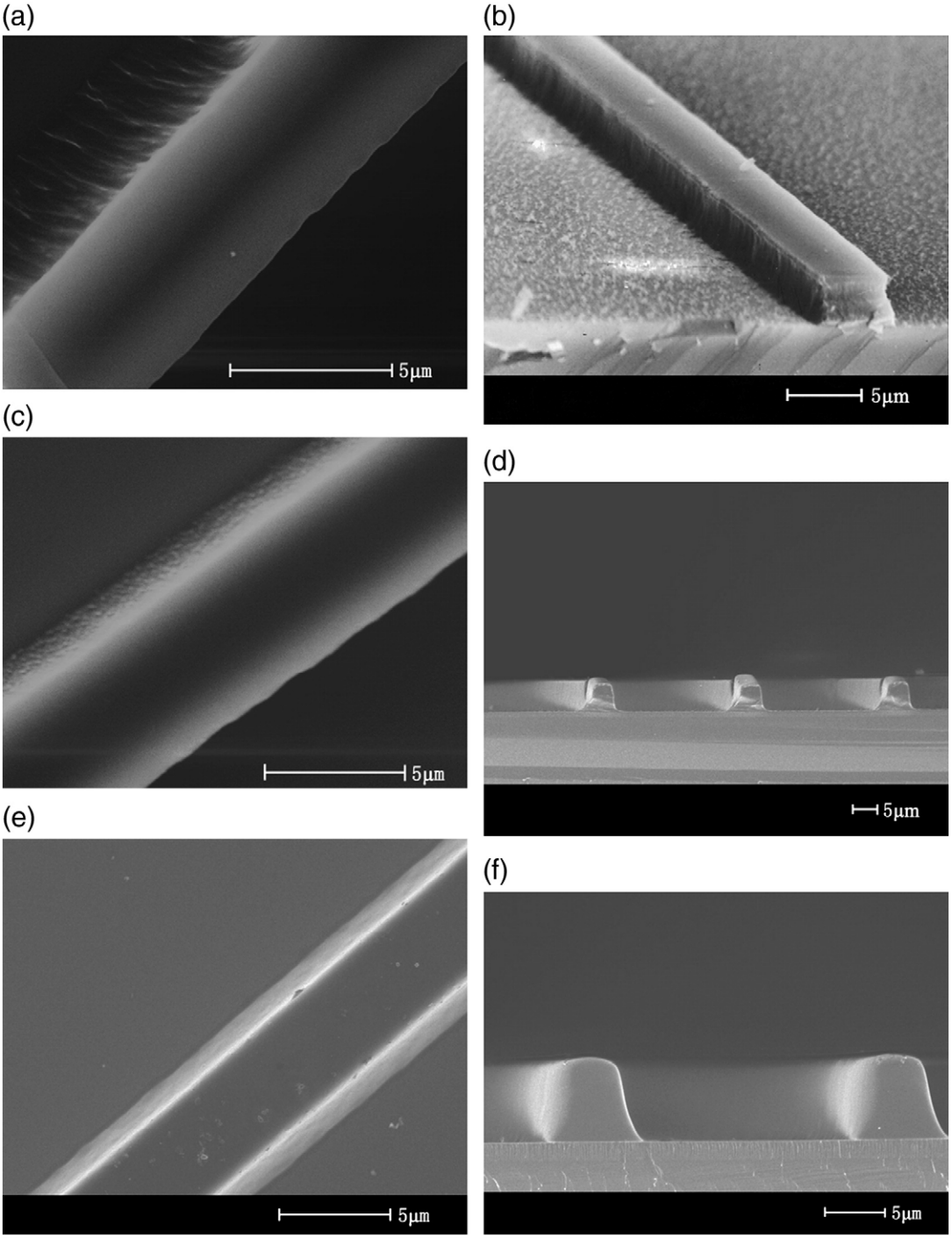

Fig. 4. SEM pictures showing the sidewall of AWG waveguides before redissolving (a) and after redissolving at 45 °C for 45 min (c), and at 55 °C for 35 min (e). The corresponding cross-sectional SEM pictures are shown in (b), (d), and (f), respectively.

expected to significantly influence the optical characteristics of AWG devices. On the other hand, if the vapor temperature is too high and the redissolving time is too long, the waveguide shape can change from a square to a trapezoid. Therefore, the redissolving temperature and time should be chosen carefully to avoid severe waveguide deformation.

To further verify the effectiveness of this technique on reducing the surface roughness scattering, waveguide loss of buried straight PFS-co-GMA waveguides with 5×5 μm^2 is measured by using a cut-back method after VRD under different conditions. The measured waveguide loss coefficient is plotted as a function of the redissolving temperature in Fig. 5. From Fig. 5 we can observe a strong relation between the reduction in the waveguide loss and the redissolving temperatures and times. Fig. 5 shows a loss reduction of 2.1 dB/cm after 35 min redissolving treatment at 55 °C. For straight waveguides, the waveguide loss mainly results from the material absorption, the substrate leakage and the sidewall roughness scattering. The

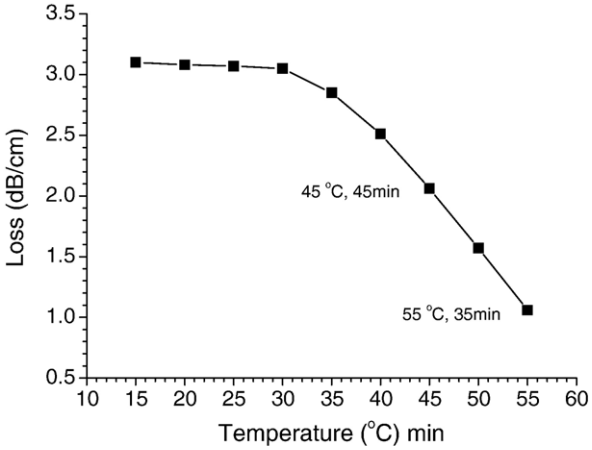

Fig. 5. Propagation losses depending on the vapor temperature for different durations, indicating the effectiveness of VRD technique in reducing the waveguide loss.

substrate leakage loss and the material absorption are independent of VRD. In order to realize the minimum substrate leakage loss, i.e. 0.01 dB, we spin and coat the lower cladding for two times and increase its thickness to 12 μm. Therefore, the variation of the waveguide loss mainly comes from that of the sidewall loss. Clearly, the waveguide loss starts to decrease above a threshold temperature and then reduces further at higher temperatures. The results demonstrate that the VRD technique can reduce the sidewall scattering loss in polymer waveguide devices very effectively.

We further measure and discuss the spectrum of the presented 33×33 AWG devices before and after the vapor-redissolving at 55 °C for 35 min. The central wavelength and wavelength spacing of our AWG device are designed to be 1550.918 nm and 0.8 nm, respectively. Fig. 2 shows the schematic layout of the designed AWG device, which consists of 33 input/output (I/O) channels, two focusing slab waveguides, and 201 arrayed waveguides, and they are all integrated on a silicon substrate. The device size is about 3.2×1.9 μm^2. The optimized values of parameters of the presented AWG are listed in Table 1. The spectral transmission characteristics of AWG are measured by using a dense wavelength division multiplexing passive component intelligent test system (IQS-510P, EXFO). Fig. 6 shows the variation of insertion loss and crosstalk before and after VRD. We can find from Fig. 6a that the crosstalk level is below −22.5 dB after vapor-redissolving at 55 °C for 35 min, and the insertion loss is between 8.5 dB for the central channel and 10.8 dB for the edge channels. Fig. 6b shows the crosstalk and insertion loss of initial AWG before VRD is about 14.0–17.5 dB and −20 dB, respectively. This indicates that the VRD technique can greatly reduce the insertion loss and crosstalk of AWG by 5.5–6.7 dB and −2.5 dB, respectively. Furthermore, the central wavelength is from 1550.96 nm to 1550.93 nm, i.e. a shift of 0.03 nm. This means that the wavelength shift is mainly result from the waveguide slight deformation.

Finally, we need to point out that the reduction of sidewall scattering loss in AWG is smaller than that in straight waveguides under the same VRD condition because solvent molecules can more easily absorb and get into the sidewalls of straight waveguides. Such a difference is due to their different structures. Obviously, the structure of the straight waveguide is much simpler than that of an AWG. The channels and arrayed waveguides of

Table 1
Optimized values of parameters of the polymer AWG multiplexer

Central wavelength	λ_0	1550.918 μm
Wavelength spacing	$\Delta\lambda$	0.8 nm
Refractive index of polymer core	n_1	1.4704
Refractive index of polymer cladding	n_2	1.463
Core width	a	5 μm
Core thickness	b	5 μm
Pitch of adjacent waveguides	d	15.5 μm
Diffraction order	m	56
Focal length of slab	f	7838.22 μm
Length difference of adjacent arrayed waveguide	ΔL	59.29 μm
Free spectral range	FSR	27.58 μm
Number of I/O channels	$2N+1$	33
Number of arrayed waveguides	$2M+1$	201

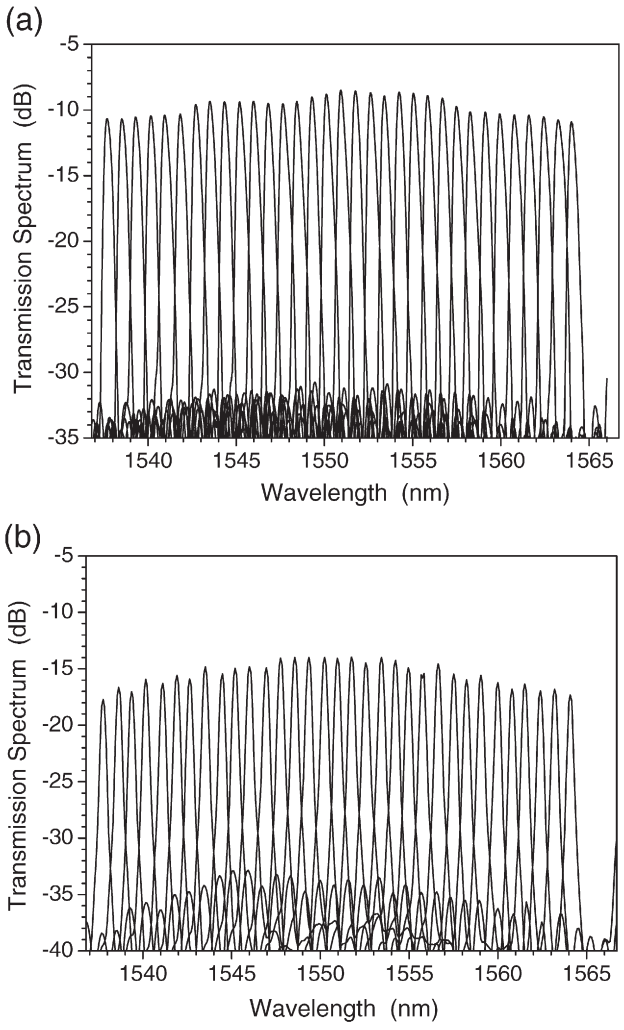

Fig. 6. Measured spectra of polymer AWG (a) with 55 °C redissolving for 35 min, and (b) without VRD treatment.

AWG are very compactly, and the solvent molecules must have larger kinetic energy to get into the sidewalls of every channel and arrayed waveguide. Therefore, the sidewall scattering loss of AWG needs to be further reduced by improving VRD technique in our future work.

In our current design of the presented AWG, the coupling loss has not been optimized. This results in the remaining loss of 3 dB. Introducing a single-mode fiber and refractive index matching liquor, we expect that the coupling loss can be reduced to minimal. With the aid of the VRD technique, we can anticipate to achieve insertion loss below 5 dB, which will lead to AWG with better multi/demultiplexing characteristics.

3. Conclusion

In summary, the VRD technique can greatly smooth the sidewalls of polymer waveguides, and reduce the sidewall scattering and further reduce the insertion loss and crosstalk of polymer AWG, which is demonstrated by SEM characterization and waveguide loss measurement. The variation of the insertion loss of the presented polymer AWG is about 5.5–6.7 dB, and that of the crosstalk is about 2.5 dB before and after VRD. In principle, the VRD technique can be applied to many other polymer waveguide devices to achieve smoother sidewall and less scattering loss. In the future research, we will improve the VRD to further reduce the sidewall scattering loss and fabricate better polymer AWG devices.

Acknowledgment

The authors wish to express their gratitude to the National Basic Research Program (973 Program) of China (2006CB302803), the National Science Foundation Council of China (60576045, 60507004) for their generous support to this work.

References

[1] K.M. Jia, W.H. Wang, Y.Z. Tang, Y.R. Yang, J.Y. Yang, X.Q. Jiang, Y.M. Wu, M.H. Wang, Y.L. Wang, IEEE Photonics Technol. Lett. 17 (2005) 378.
[2] S. Kamei, K. Iemura, A. Kaneko, Y. Inoue, T. Shibata, H. Takahashi, A. Sugita, IEEE Photonics Technol. Lett. 17 (2005) 588.
[3] L. Eldada, L.W. Shacklette, IEEE J. Sel. Top. Quantum Electron. 6 (2000) 54.
[4] E.S. Kang, W.S. Kim, D.J. Kim, B.S. Bae, IEEE Photonics Technol. Lett. 16 (2004) 2625.
[5] I. Molina-Fernández, J.G. Wangüemert-Pérez, Opt. Express 12 (2004) 4804.
[6] V. Van, P.P. Absil, J.V. Hryniewicz, P.T. Ho, J. Lightwave Technol. 19 (2001) 1734.
[7] D.K. Armani, T.J. Kippenberg, S.M. Spillane, K.J. Vahala, Nature 421 (2003) 925.
[8] S. Toyoda, N. Ooba, A. Kaneko, M. Hikita, T. Kurihara, T. Maruno, Electron. Lett. 36 (2000) 658.
[9] N. Keil, H.H. Yao, C.A. Zawadzki, Electron. Lett. 37 (2001) 579.
[10] C.Y. Yen, L.J. Guo, Appl. Phys. Lett. 84 (2004) 2479.
[11] F. Wang, C.S. Ma, W. Sun, A.Z. Li, Y. Zhao, Z.H. Jiang, D.M. Zhang, Opt. Laser Technol. 37 (2005) 527.
[12] C.S. Ma, H.M. Zhang, D.M Zhang, Z.C. Cui, S.Y. Liu, Opt. Commun. 241 (2004) 321.